# Copper Electroless Process Optimization to Modify Boron Doped Diamond at Different Boron Levels

C.F. Pereira, A.B. Couto, M.R. Baldan, N.G. Ferreira

Instituto Nacional de Pesquisas Espaciais, São José dos Campos, Brasil.

The copper electroless deposition on semiconducting boron doped diamond (BDD) grown on Ti substrate was investigated. This study emphasizes the influence of the doping level on BDD in the Cu electroless process. In addition, the effect of some deposition parameters such as the pH solution and the deposition time, to obtain Cu/BDD composites were analyzed. Two kinds of BDD films were produced and named as lightly (E1) and highly (E2) BDD electrodes. For both Cu/BDD composites, the scanning electron microscopy showed the deposit morphologies composed by small grains distributed throughout the BDD surface when the electroless process was conducted at pH 12. On the other hand, no Cu deposit was verified at pH 8 and pH 10 for deposition times up to 180 s. However, in these conditions, low particle density was observed for deposition time of 2400 s. In general, the Cu deposit rate increased with increasing the deposition time, for both BDD films. The influence of doping level showed that for E2 electrode, the deposits presented higher density and better uniformity of Cu particle on its surface than those for E1 electrode. This behavior may be associated to the better conductivity of the E2 electrode due to its higher boron content enhancing the Cu deposition. According the X-ray diffraction data, the Cu metallic crystallographic form was obtained for all deposited particles.

## Introduction

The monitoring of nitrate ion is of great worldwide interest, because elevated concentration of this specie on ground water is directly associated to a high number of ecological and human health concerns [1-3]. Cu/BDD composites have shown high potential to use as solid electrode for application in environmental approaches [4]. Particularly, the copper exhibits high electrocatalytic activity considering the kinetics for the nitrate reduction process. Thus, Cu/BDD composites have appeared as potential material to study the nitrate removal from the polluted waters [5]. There are many ways to produce Cu/BDD composites by diverse routes such as, photoelectrodeposition process [6], sputtering [7], electrodeposition [8], physical vapor deposition (PVD) [9], wetness technique [10], and electroless deposition [11]. Among them, the electroless plating has emerged in latter years due to its low cost, fast deposition rate and good filling capability. In addition, its major advantage is its simplicity, where the processes can take place at room temperatures and pressures [12].

Considering Cu electroless process, the BDD chemical inertness may contributes to a low Cu adherence. Therefore, a hard pre-treatment is needed for cleaning the surface and creating anchor points on the BDD samples [13]. These anchor points are oxygen groups that appear on the BDD surface, such as, hydroxyl (O-H), carboxylic (C=O) and carbonylic (C-O). The oxidative pre-treatments can be obtained using different techniques, like oxygen plasma [14], boiling in strong acids [15], ozone exposure [16] and electrochemical oxidation [17]. In this study, the anodic electrochemical pre-treatment was carried out using 0.5 mol $L^{-1}$ $H_2SO_4$ and a fixed potential of 3 V for 30 min. This type of pre-treatment is recognized as an effective method of treatment which is able to functionalize diamond surface. Besides, it can be conducted under controlled treatment time. In this sense, this paper investigates the influence of the BDD doping level in the Cu electroless synthesis as well as the effect of some deposition parameters such as the solution pH and the deposition time, to obtain Cu/BDD composites.

## Experimental Procedure

The BDD electrode was grown on Ti substrate by hot filament chemical vapor deposition (HFCVD) technique. The deposition of diamond on titanium has a unique feature attributed to the strong stress formation between the film and the substrate, which arises from extrinsic and intrinsic factors. Thus, some pre- treatments on the substrate surface are required to decrease the stress and to increase the nucleation rate [18, 19]. These pre-treatments can be obtained in air abrasion with glass beads, or by scratching the surface with an abrasive agent as the diamond paste. In the present work, the films were deposited on the titanium substrate after pre-treatment in air abrasion with glass beads. The BDD/Ti electrodes with the dimensions of 10 mm x 10 mm x 0.5 mm were prepared from methane hydrogen gas mixture with a pressure of 40 Torr and temperature around 650ºC, during 24 h. Boron source was obtained by an additional hydrogen line passing through a bubbler containing $B_2O_3$ dissolved in methanol with a controlled B/C ratio that permitted to produce films with different doping levels (5000 and 15000 ppm), denominated E1 and E2 respectively), estimated from Raman's measurements. Prior to the Cu electroless deposition, the sensitization on the BDD was achieved using a solution of 40 mL $L^{-1}$ HCl containing 0.04 mol $L^{-1}$ $SnCl_2$ for 5 min and the activation was made using a solution containing $7x10^{-4}$ mol $L^{-1}$ $PdCl_2$ with 2.5 mL $L^{-1}$ HCl for 5 min. Ultrasonic vibration was used for both steps. The electroless Cu deposition was carried out for different times (30, 60, 180 and 2400 s) at room temperature. The bath composition was 0.1 mol $L^{-1}$ $CuSO_4$ + 0.2 mol $L^{-1}$ $KNaC_4H_4O_6$ + 17.5 mL $L^{-1}$ HCHO. The pH level was adjusted to 8, 10 and 12 by the addition of NaOH. Fourier transform infrared (FTIR) spectrometer with attenuated total reflectance (ATR) Model Spectrum 100 from Parkin Elmer equipment was used to monitor the anchor points associated with the functional groups on BDD surfaces promoted by the pre-treatments. The Cu modified diamond films morphology was verified from the scanning electron microscopy (SEM) images using a Jeol JSM-5310 microscope and the X-ray Diffraction (XRD) patterns using a PANanalytical model X'Pert Powder diffractometer with the CuKα (λ = 1.54 Å), set at 45 kV and 25 mA, running in the ω/2θ scanning mode with ω = $1^o$ and 2θ = 10 to $100^o$.

## Results and discussion

Figure 1 shows the Raman scattering spectra of E1 and E2 BDD films. The peak close to 1332 $cm^{-1}$ corresponds to the vibration of a diamond first-order phonon, confirming the quality of these BDD films. This peak decreased in intensity due to boron incorporation in diamond films. The effect of boron doping is reflected in the spectral characteristics. There is the appearance of the two bands located at 500 $cm^{-1}$ and 1220 $cm^{-1}$ attributed to B-B vibrations and B-C vibrations, respectively [20]. The boron concentration in diamond film was estimated from the fitting of 500 $cm^{-1}$ peak using a combination of Gaussian and Lorenzian lines [21]. The acceptor concentrations were evaluated around $10^{19}$ and $10^{21}$ boron atoms $cm^{-3}$ for E1 and E2 electrodes, respectively. The difference of doping level for E2 electrode is clearly noted in Raman spectra, where the 500 and 1220 $cm^{-1}$ bands are much more pronounced.

The top view SEM images (not shown) of the diamond film deposited on the Ti substrates showed that the BDD films grew with a continuous and uniform surface morphology covering the whole substrates without delaminations or cracks, characterized by their well-shaped microcrystalline grains.
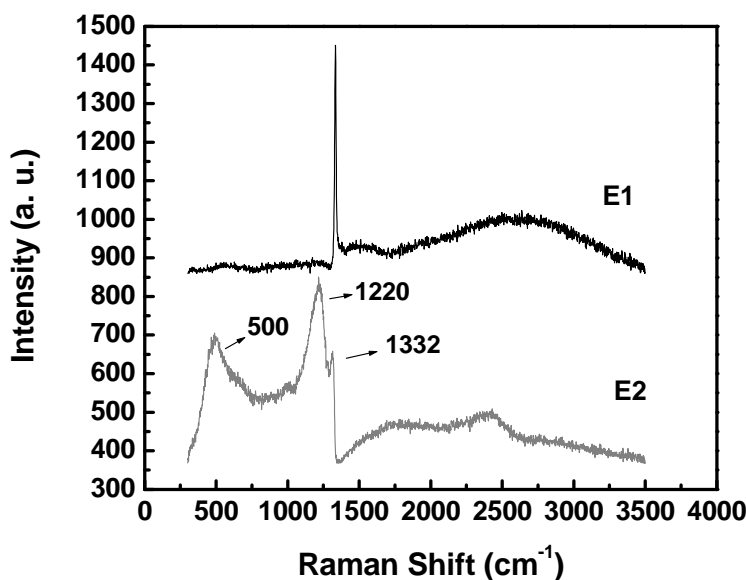


**Figure 1:** Raman spectra of E1 and E2 BDD electrodes.

According to the literature, as-grown diamond surface obtained by hot filament-assisted chemical vapor deposition technique is mainly a hydrogen terminated surface [22]. The change in the surface atomic structure can be obtained using different oxidation processes. In this study the anodic electrochemical pre-treatment was carried out using 0.5 mol $L^{-1}$ $H_2SO_4$ and a fixed potential of 3 V for 30 min. FTIR-ATR analysis was made to evaluate the chemical surface after electrochemical pre-treatments regarding the presence of oxygen functional groups on the BDD surfaces for both studied electrodes. Fig.2 shows the FTIR-ATR graph analyzes of E2 BDD electrode before and after electrochemical pre-treatment. Similar behavior was observed for E1 BDD electrode (not shown).
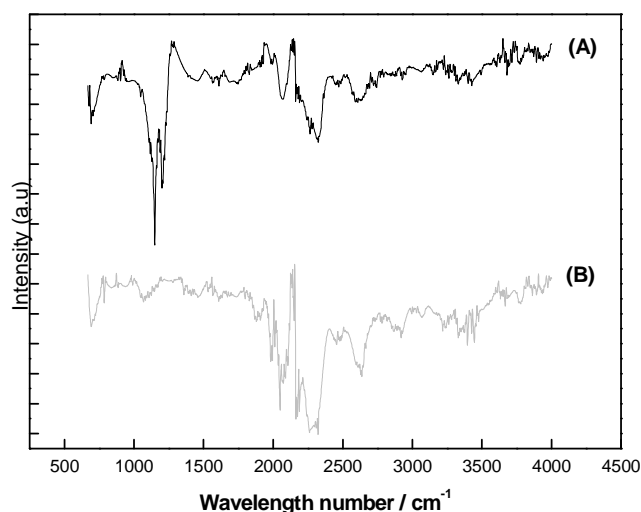
**Figure 2:** FTIR-ATR results with peaks identified for E2 BDD electrode: (A) after electrochemical pre-treatment, (B) without electrochemical pre-treatment.

According to Fig.2, the FTIR-ATR results presented a slight difference between the E2 BDD electrode without and after electrochemical pre-treatment. However, the 1000-1260 cm$^{-1}$ range, corresponding to the functional group (C-O), was more pronounced after anodic electrochemical pre-treatment. This behavior may be associated to the oxygenated functional group formations, i.e, ether, ketone and carboxylic acid groups due to the applied oxidative process. It is noteworthy that neither SEM images nor Raman spectra showed no significant change in the diamond surfaces after anodic electrochemical pre-treatment (not shown), which indicated that the pre-treatment did not impair the crystal quality and the morphology of the BDD surface. These results are in agreement with the literature that discuss only the diamond functionalization process promoted by oxidative pre-treatments [23].

The top view SEM images of the electroless Cu deposits on BDD surface as a function of pH are depicted in Figure 3.
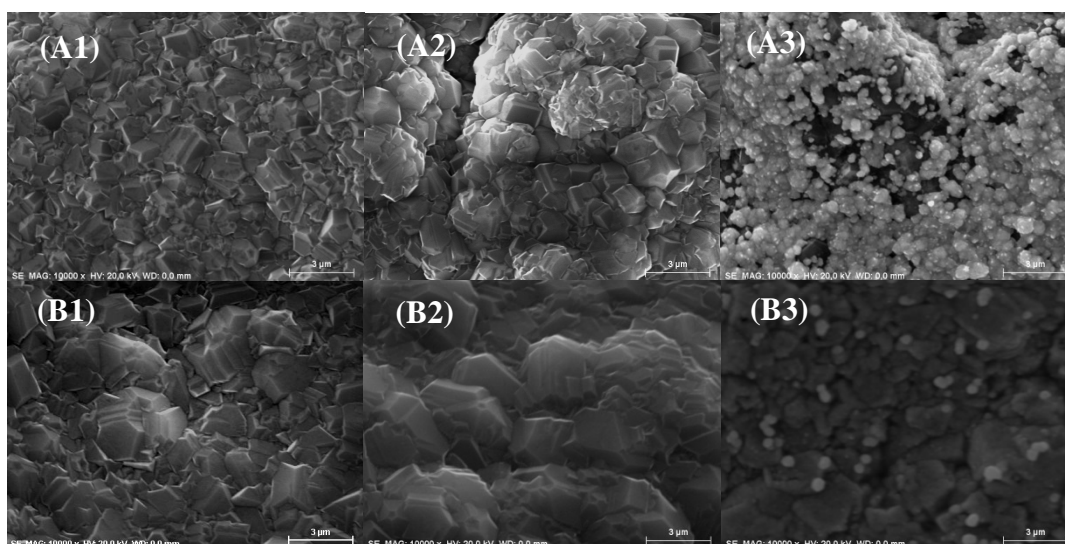
**Figure 3:** SEM images of E1 (A) and E2 (B) BDD electrode after Cu deposits as a function of pH: pH 8(A1, B1), pH 10 (A2, B2) and pH 12 (A3, B3). Deposition time: 180 s.

According to Scanning Electron Microscopy images the Cu deposits showed small grain particle distribution on the BDD surface for solution of pH 12. Image A3 presents BDD not totally covered by Cu particle while for image B3 the BDD is totally covered with a Cu clusters over the Cu layer. The EDS data indicate that the Cu content was 77.36 wt.% for E2 electrode (image B3) whereas the Cu content was 69.20 wt.% for E1 electrode (image A3). On the other hand, no Cu deposit was verified at pH 8 and at pH 10 in the range of deposition time from 30 to 180 s and only low particle density was observed for deposition time of 2400 s, for both electrodes. In this deposition time, the EDS measurements indicate that in the pH 8 the Cu content was 5.87 wt.% whereas in the pH 10 the Cu content was 7.73 wt.% for E2 electrode. Similar experimental conditions for electroless Cu deposition on E1 electrode showed the same behavior as a function of pH. This behavior can be explained considering the electroless coating process, which Cu cations capture electrons furnished by HCHO, they are reduced and deposited onto the BDD surface as Cu metallic by following chemical reactions:

$$HCHO + OH^- \rightarrow H_2 + HCOO^-$$
$$Cu^{2+} + 2\ HCOO^- + 3\ H_2 \rightarrow Cu + 2\ HCHO + 2\ H_2O$$
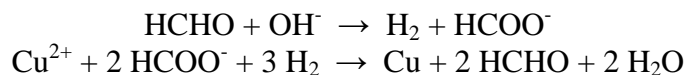
Thus, the overall reaction can be written as:

$$Cu^{2+} + H_2 + 2\ OH^- \rightarrow Cu + 2\ H_2O$$

According to the above reactions, it is possible to observe that the reducing power of HCHO increases with increasing the solution pH. As a consequence, higher Cu deposits were observed in the pH 12.

Figure 4 shows the SEM micrographs of E1 and E2 electrodes after surface modifications of Cu particles, using pH 12 and varying the deposition time of 30, 60 and 180 s.
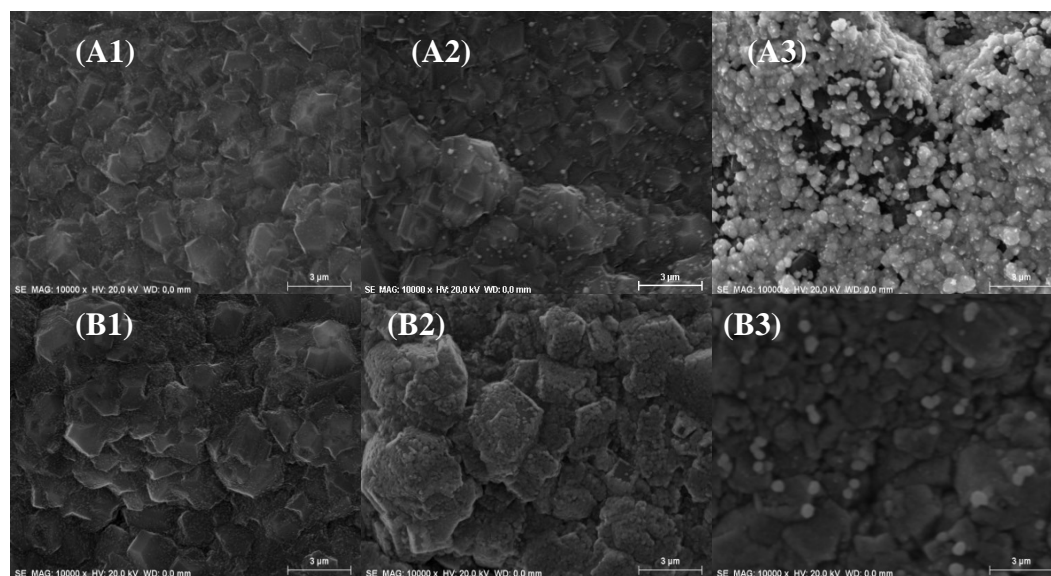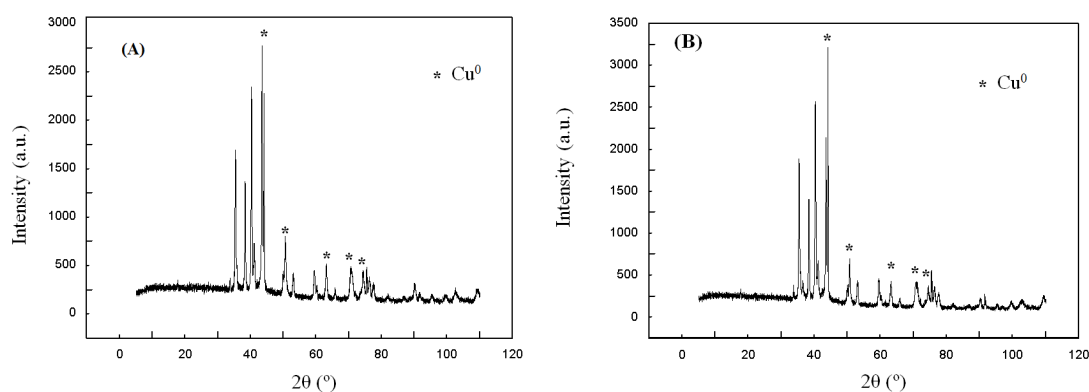
**Figure 4:** SEM images of E1 (A) and E2 (B) BDD electrode after Cu deposits. Deposition time: 30 s (A1, B1), 60 s (A2, B2) and 180 s (A3, B3).

These deposits depict small grain morphologies distributed throughout the BDD surface for both electrodes. The Cu deposit rate increased with increasing the deposition time, for both BDD films. From EDS measurements, the Cu contents as a function of deposition times of 30, 60 and 180 s were 7.94, 27.74 and 77.36 wt.% for E2 BDD electrode while for E1 BDD electrode they were 1.87, 18.44 and 69.20 wt.%, respectively. By comparing these results for both electrodes, higher deposition rates were observed in the E2 electrode. This morphological difference between two electrodes, concerning the Cu deposit densities, can be attributed to the better conductivity of the electrode E2 due to its higher boron content.

Figure 5 presents the X-ray diffraction measurements of the Cu deposited on E1 and E2 BDD electrode. According to the patterns, the Cu metallic crystallographic form was obtained for all deposits, as expected.



**Figure 5:** X-ray diffraction of E1 (A) and E2 (B) BDD electrode after the Cu deposition, at pH 12 and for 180 s deposition time.

## Conclusion

This study showed that the Cu electroless process on semiconducting diamond surface can be a good alternative for obtaining modified electrode at different doping levels. The Cu deposits presented small grains morphology distributed all over the diamond crystal faces for both electrodes depend on the electrode boron level, solution pH, and deposition time. The Cu metallic crystallographic form was obtained for all the depositions. The Cu deposits increased with increasing the pH solution. SEM images showed a high density of Cu electrodeposits for highly doped BDD electrode whereas for lightly doped BDD electrode the deposits presented low particle density. This behavior was attributed to the higher conductivity of the E2 BDD electrode.

## Acknowledgments

## References

[1] K. H. Gelberg, L. Church, G. Casey, M. London, D. S. Roerig, J. Boyd, M. Hill, Nitrate levels in drinking water in rural New York State, Environ. Res. 80 (1999) 34-40.

[2] Archna, Surinder K. Sharma, Ranbir Chander Sobti, Nitrate removal from ground water: a review, E-Journal of Chemistry 9(4) (2012) 1667-1675.

[3] Inam-Ul-Haque, Muqaddas Tariq, Electrochemical reduction of nitrate: a review, J. Chem. Soc. Pak. 32 (2010) 396-418.

[4] G.E. Dima, A.C.A. Vooys, M.T.M. Koper, Electrocatalytic reduction of nitrate at low concentration on coinage and transition-metal electrodes in acid solutions, J. Electroanal. Chem. 554 (2003) 15-23.

[5] F. M. M. Paschoal, L. Nuñez, M. R. V. Lanza, M. V. B. Zanoni, Nitrate removal on a Cu/Cu$_2$O photocathode under UV irradiation and bias potential, J. Adv. Oxid. Tecnol. 16 (2013) 63-70.

[6] S. Yoshihara, K. Shinozaki, T. Shirakashi, K. Hashimoto, D.A. Tryk, A. Fujishima, Photoelectrodeposition of copper on boron-doped diamond films: application to conductive pattern formation on diamond. The photographic diamond surface phenomenon, Electrochimica Acta 44 (1999) 2711-2719.

[7] E. Neubauer, G. Korb, C. Eisenmenger-Sittner, H. Bangert, S. Chotikaprakhan, D. Dietzel, A.M. Mansanares, B.K. Bein, The influence of mechanical adhesion of copper coatings on carbon surfaces on the interfacial thermal contact resistance, Thin Solid Films 433 (2003) 160-165.

[8] S. Arai, M. Endo, Carbon nanofiber–copper composite powder prepared by electrodeposition, *Electrochemistry Communications* 5 (2003) 797-799.

[9] C. Schrank, C. Eisenmenger-Sittner, E. Neubauer, H. Bangert, A. Bergauer, Solid state de-wetting observed for vapor deposited copper films on carbon substrates, Thin Solid Films 459 (2004) 276-281.

[10] J. Ma, C. Park, N.M. Rodriguez, R.T.K. Baker, Characteristics of Copper Particles Supported on Various Types of Graphite Nanofibers, J. Phys. Chem. B 105 (2001) 11994-12002.

[11] W. Lu, V.S. Donepudi, J. Prakash, J. Liu, K. Amine, Electrochemical and thermal behavior of copper coated type MAG-20 natural graphite, Electrochim. Acta 47 (2002) 1601-1606.

[12] J. Tamayo-Ariztondo, J. M. Córdoba, M. Odén, J. M. Molina-Aldareguia, M. R. Elizalde, Composites Science and Technology 70, (2010) 2269-2275.

[13] F. Wang, S. Arai, M. Endo, Metallization of multi-walled carbon nanotubes with copper by electroless deposition process, Electrochem Commun 6 (2004) 1042-1044.

[14] E.D. Perakslis, S.D. Gardner, C.U. Pittman, Surface Composition of Carbon Fibers Subjected to Oxidation in Nitric Acid Followed by Oxygen Plasma, J. Adhes. Sci. technol. 11 (1997) 531-551.

[15] J.M. Córdoba, M. Odén, Growth and characterization of electroless deposited Cu films on carbon nanofibers, Surface & Coatings Technology 203 (2009) 3459-3464.

[16] X. Fu, W. Lu, D.D.L. Chung, Ozone treatment of carbon fiber for reinforcing cement, Carbon 36 (1998) 1337-1345.

[17] B. Lindsay, M.L. Abel, J.F. Watts, A study of electrochemically treated PAN based carbon fibres by IGC and XPS, Carbon 45 (2007) 2433-2444.

[18] S.J. Askari, F. Akhtar, G.C. Chen, Q. He, F.Y. Wang, X.M. Meng, F.X. Lu, Materials Letters 61 (2007) 2139-2142.

[19] A.F. Azevedo, E.J. Corat, N.F. Leite, V.J. Trava-Airoldi, Diamond Related Materials 11 (2002) 550-554.

[20] Li Niu, Jia-Qi Zhu, Xiao Han, Man-Lin Tan, Wei Gao, Shan-Yi Du, Physics Letter A 373 (2009) 2494-24500.

[21] M. Bernard, A. Deneuville, P. Muret, Diamond Related Materials 13 (2004) 282-286.

[22] S. Szunerits, R. Boukherroub, Different strategies for functionalization of diamond surfaces, J. Solid State Electrochem. 12 (2008) 1205-1218.

[23] M. Wang, N. Simon, C. Decorse-Pascanut, M. Bouttemy, A. Etcheberry, M. Li, R. Boukherroub, S. Szunerits, Comparison of the chemical composition of boron-doped diamond surfaces upon different oxidation processes, Electrochimica Acta 54 (2009) 5818-5824.